

IMPEDANCE OPTIMIZATION OF SMALL GAP CHAMBERS FOR THE HIGH SINGLE BUNCH CURRENT OPERATION AT THE UNDULATOR BASED LIGHT SOURCES

Yong-Chul Chae[†], DESY, Hamburg, Germany

Abstract

In the undulator based light sources the intensity limit of single bunch is often determined by the strong vertical instability caused by the wake field in the ring, where the undulator itself is large impedance source. The optimization of transition from the large aperture to undulator's small-gap chamber is on-going research topic in an effort to reduce the vertical impedance; at the same time, the demand on single-bunch current is high from the timing-mode x-ray user community. In this paper, after showing the results obtained by exploring the parameter space guided by Stupakov's formula, we propose the linearly-segmented transition which can reduce the impedance down to 60% or less of the original linear taper. The reduction can be utilized either to increase the bunch current substantially or to install a smaller gap chamber without impacting the bunch current limit. For the definite result we considered the transition between two ellipses, namely, $(a, b) = (42 \text{ mm}, 21 \text{ mm})$ and $(18 \text{ mm}, 4 \text{ mm})$ over the length 15-30 cm in beam direction.

INTRODUCTION

In the 3rd generation light source the demand in high single bunch current often requires a strict control of impedance. The moderate change in impedance can have significant impact on the single bunch current limit. Main impedance source is insertion device (ID) chamber with a small gap. In this paper we present the impedance optimization of ID chamber taking into account of linear and nonlinear transition, width and gap of ID chamber, super-ellipse parameter of cross section, and the symmetry breaking of upstream and downstream transition. Specifically, we like to make vertical impedance of the transition between two ellipses, namely, $(a, b) = (42 \text{ mm}, 21 \text{ mm})$ and $(18 \text{ mm}, 4 \text{ mm})$ to be small. This is the reference configuration with the transition length equal to 18 cm. Most of the optimization result is normalized by this reference case.

LINEAR TAPER OPTIMIZATION WITH CONSTRAINT

Let's consider a transition between arc and ID chamber as shown in Fig. 1. We firstly set the value of b to 17 mm or 21 mm. For each value of b , we varied the horizontal aperture a in wide range from 42 mm down to 10 mm. The vertical kick factor computed by the program GdfidL [1] is shown in Fig. 2 as a function of a . The results are normalized by the reference case. There is a significant reduction in K_y as the upstream aperture of taper gets

smaller. However, this design makes rf heating large because of the abrupt change in aperture. The new design is proposed in Fig 3, which results in the significantly reduced rf heating. Overall reduction in vertical impedance is 45% when $a=b=17 \text{ mm}$ is used.

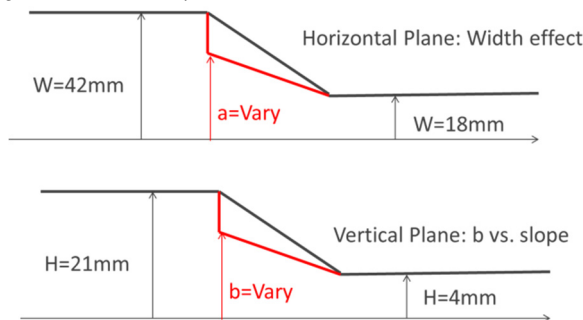


Figure 1: The linear taper connecting arc and ID chambers showing the horizontal plane (top) and the vertical plane (bottom). Black curve represents the profile of the reference chamber and the red curve indicates a new profile with optimization parameters a and b .

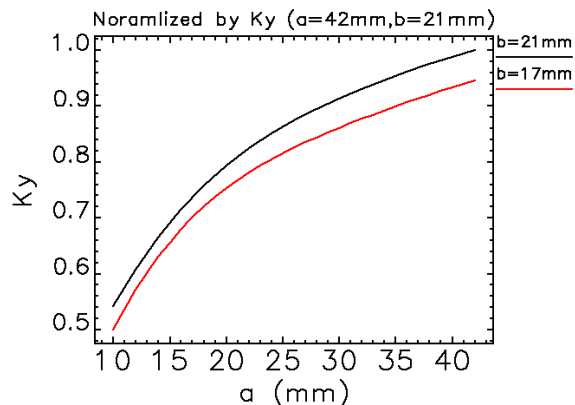


Figure 2: The reduction of vertical kick factor as the horizontal aperture, a , reduces from the original 42 mm down to 10 mm for a given vertical aperture, b .

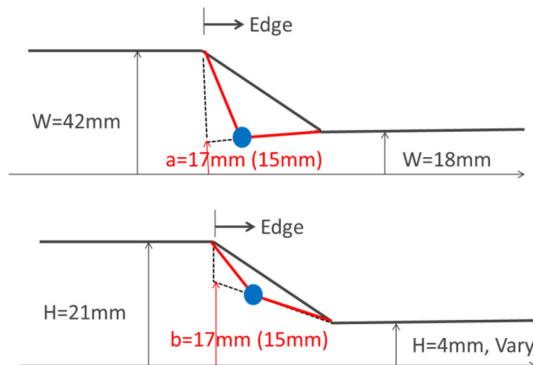


Figure 3: The optimized linear taper which is similar to Fig. 1 but with two segmented transitions.

[†] yong-chul.chae@desy.de

Content from this work may be used under the terms of the CC BY 3.0 licence (© 2018). Any distribution of this work must maintain attribution to the author(s), title of the work, publisher, and DOI.

TAPER OPTIMIZATION WITHOUT CONSTRAINT

ID Chamber Profile

It was Yokoya who found that the wake for hyperbolic pipe is considerably smaller than that for the round pipe in the short-range region if the wall is resistive [2]. We considered the ID chamber whose cross-section is a super-ellipse which is defined as:

$$\left| \frac{x}{a} \right|^n + \left| \frac{y}{b} \right|^n = 1, \quad (1)$$

where a and b are the semi-axis of ellipse and, depending the parameter n , the curve is called hypo-ellipse if $n > 2$, ellipse if $n = 2$ and hyper-ellipse if $n < 2$. The curves of different n are shown in Fig. 4. For n goes to infinity, the curve becomes a rectangle. The program GdfidL modelled a linear transition from the regular ellipse of (42 mm, 21 mm) to super-ellipse of (18 mm, 4 mm). The vertical wake was computed and its result was normalized by the reference ID chamber with $n = 2$. The resultant kick factor for different values of n is shown in Fig. 5. The smallest wake occurs at the rhombus ($n = 1$) and then increase very quickly to high value for $n < 1$. On the other hand, for $n > 2$, the wake grows slowly approaching asymptotic value toward the rectangle. The rectangular chamber has advantage in terms of large injection aperture but it has larger impedance than elliptic chamber by 20% as shown in Fig. 5.

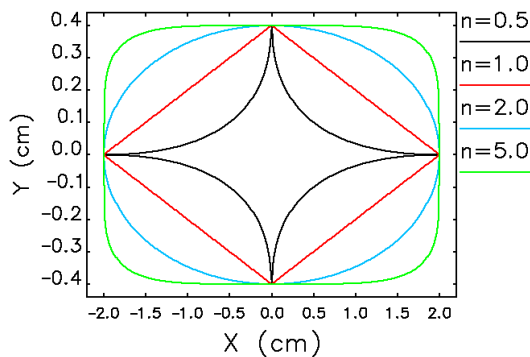


Figure 4: Curves of super-ellipse for different values of n .

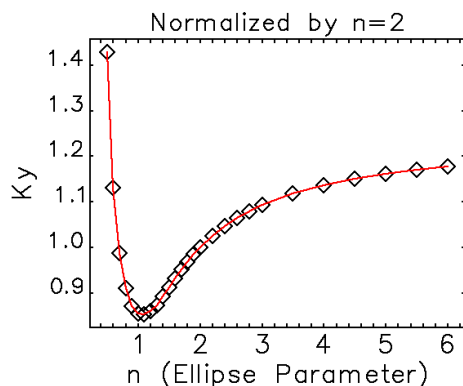


Figure 5: Vertical kick-factor as a function of super-ellipse parameter n .

Symmetric vs. Asymmetric Linear Transition

When the cross-section of arc and ID chamber is fixed, then the taper length can be an optimization parameter. A general transition is depicted in Fig. 6, where L_1 and L_2 denote the taper length and β_1 and β_2 are the lattice function which is the weight applied to the impedance.



Figure 6: Transition with different length and lattice function.

For the symmetric transition where $L_1 = L_2 = L$ and $\beta_1 = \beta_2 = \beta$ the length L is only parameter we can vary for optimization. For the linear transition between two ellipses of $(a, b) = (42 \text{ mm}, 21 \text{ mm})$ to $(18 \text{ mm}, 4 \text{ mm})$ over the length $L = 18 \text{ cm}$ as the reference, we varied the length L , and recorded increase and decrease of wake as a function of L . The result normalized by the reference wake is shown in Fig. 7. The symbols of different color represent different gap of ID chamber from 6 mm to 9 mm. The reference case is for 8 mm gap chamber. A practical consideration may put the limit on the taper length below 50 cm, above which we also observe the diminished return in impedance optimization.

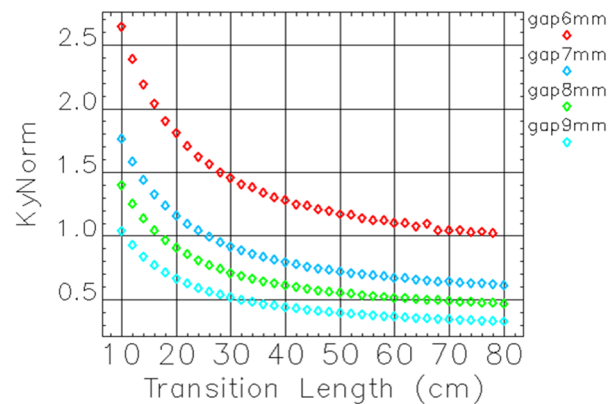


Figure 7: Transition with different length and lattice function.

However, if the constraint is set on the combined length of transition, namely on $L = L_1 + L_2$, then the total length L is fixed but L_1 or L_2 can be a free parameter. In this situation it is not so obvious whether the symmetric transition is optimum, because the wakes of taper-in and taper-out could be quite different. For a given L we varied the length of taper-in, namely, L_1 . The results obtained by GdfidL simulation is presented in Fig. 8, where the kick factor is depicted as a function of L_1 for the different values of L from 40 cm to 70 cm. The symmetric transition occurs when $L_1 = L_2 = L/2$, whose result is also included in Fig. 8 as symbols. From which we observe that the symmetric one is indeed optimum in producing the smallest wake.

Content from this work may be used under the terms of the CC BY 3.0 licence (© 2018). Any distribution of this work must maintain attribution to the author(s), title of the work, publisher, and DOI.

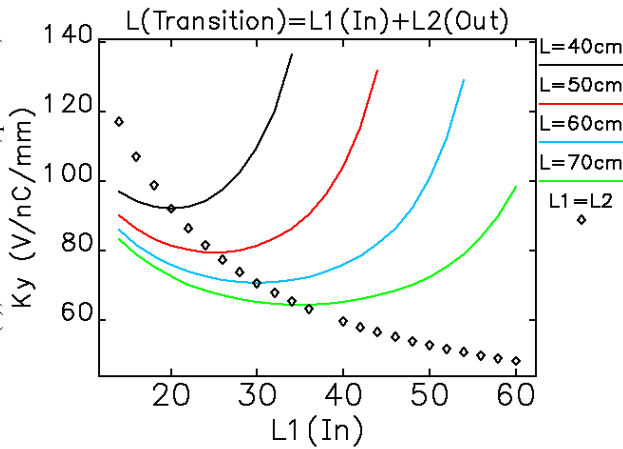


Figure 8: Transition with different length and lattice function.

Linear vs. Nonlinear Transition

At low frequency approximation the vertical impedance of rectangular chamber with constant width w is [3]

$$Z_y(k) = j \frac{Z_0 w}{4} \int_{-\infty}^{\infty} \frac{h'(z)^2}{h(z)^3} dz, \quad (2)$$

where $h(z)$ is the profile of vertical taper. The optimum profile to minimize the Z_y in Eq. (2) is found to satisfy [4]

$$h(z) = \frac{h_{\min}}{\left(1 + \left(\beta^{-1/2} - 1\right)z/L\right)^2}, \quad \beta \equiv \frac{h_{\max}}{h_{\min}}, \quad (3)$$

where h_{\min} is the half-height of ID chamber and h_{\max} is the half-height of arc chamber. In this paper h_{\min} is 4 mm and h_{\max} is 21 mm, and the nonlinear transition was approximated as many segments of short length; however, the resultant profile closely followed the analytic curve of Eq. (3). The wake potential was simulated by a short bunch, then its impedance was utilized to compute the kick factor of long bunch in any length so that we can study the range of applicability where Eq. (3) is valid.

The normalised result in comparison with the linear taper is shown in Fig. 9. For flat chamber the kick factor decreased by 20% for a long bunch if we had used nonlinear profile of Eq. (3). However, the chamber width is not constant. For the reference chamber (the APS chamber) the width varies from 42 mm to 18 mm. When we applied the same vertical profile of Eq. (3) to the APS chamber, we found no reduction in kick factor for a long bunch case. So we concluded that nonlinear transition is effective when the width is constant.

Width Effect

The vertical impedance increases linearly with the width of chamber according to Eq. (2). In order to make better decision on linear vs nonlinear transition for the smaller impedance, we had tested Eq. (2) by simulation. We used the APS chamber as the reference but the width of ID chamber was varied from 10 mm to 50 mm with respect to the nominal value of 18 mm. The result in ver-

tical kick factor is shown in Fig. 10 as a function of ID chamber width. It showed that the kick factor can be reduced by 17% by keeping 18 mm instead of 42 mm wide chamber which is necessary for nonlinear optimization to be effective.

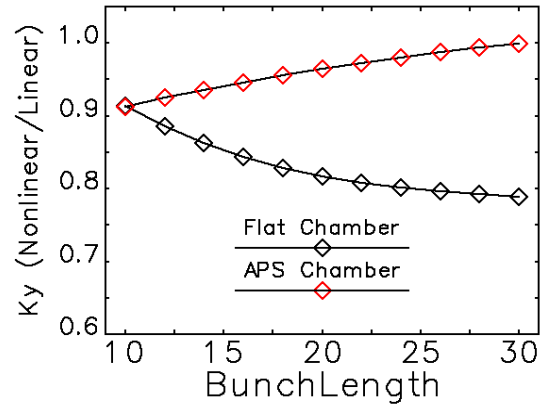


Figure 9: Vertical kick factor as a function of bunch length. Flat chamber corresponds to the constant width and the APS chamber is not constant in width.

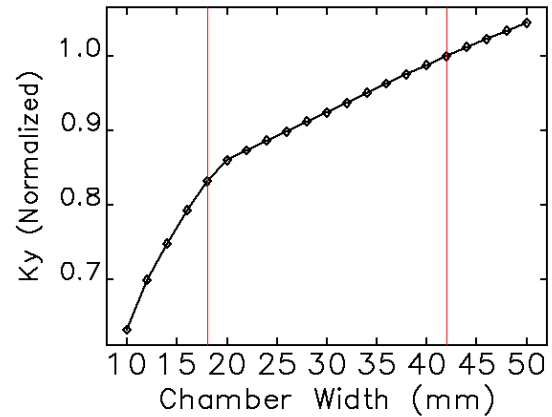


Figure 10: Vertical kick factor as a function of bunch length. Flat chamber corresponds to the constant width and APS chamber to the not constant width.

CONCLUSION

We had found a method to reduce the geometric impedance of ID chamber by a segmented taper working on the upstream side of transition where the arc chamber has large aperture. The impedance was reduced by 45% when the technique was applied to the APS chamber used as a reference.

REFERENCES

- [1] GdfidL, <http://www.gdfid1.de>
- [2] K. Yokoya, "Resistive wall impedance of beam pipes of general cross section", *Part. Accel.*, Vol. 41, pp. 221-248, 1993.
- [3] G. Stupakov, *Phys. Rev. ST Accel. Beams* 10, 094401 (2007).
- [4] B. Podobedov, I. Zagorodnov, "Impedance Minimization by Nonlinear Tapering," Proc. PAC'07, 2007, p. 2006.